

# Low-density composite powder for lightweight parts made by means powder metallurgy



**RIGA TECHNICAL UNIVERSITY**

A. Shishkin<sup>1</sup>, V. Kozlov<sup>2</sup>, M. Drozdova<sup>3</sup>, J. Rulov<sup>2</sup>, V. Mironov<sup>1</sup>, I. Hussainova<sup>3</sup>

<sup>1</sup>Riga Technical University, Laboratory of Powder Materials, Azenes Str. 16/20, lab. 331, LV – 1048, Riga, Latvia

<sup>2</sup>Sidrabe Ltd, Krustpils iela 17, Rīga, LV-1073, Latvia,

<sup>3</sup>Tallinn University of Technology, Department of Materials Engineering, Ehitajate tee 5, 19086 Tallinn, Estonia



TALLINN UNIVERSITY OF TECHNOLOGY



## MATERIALS AND METHODS

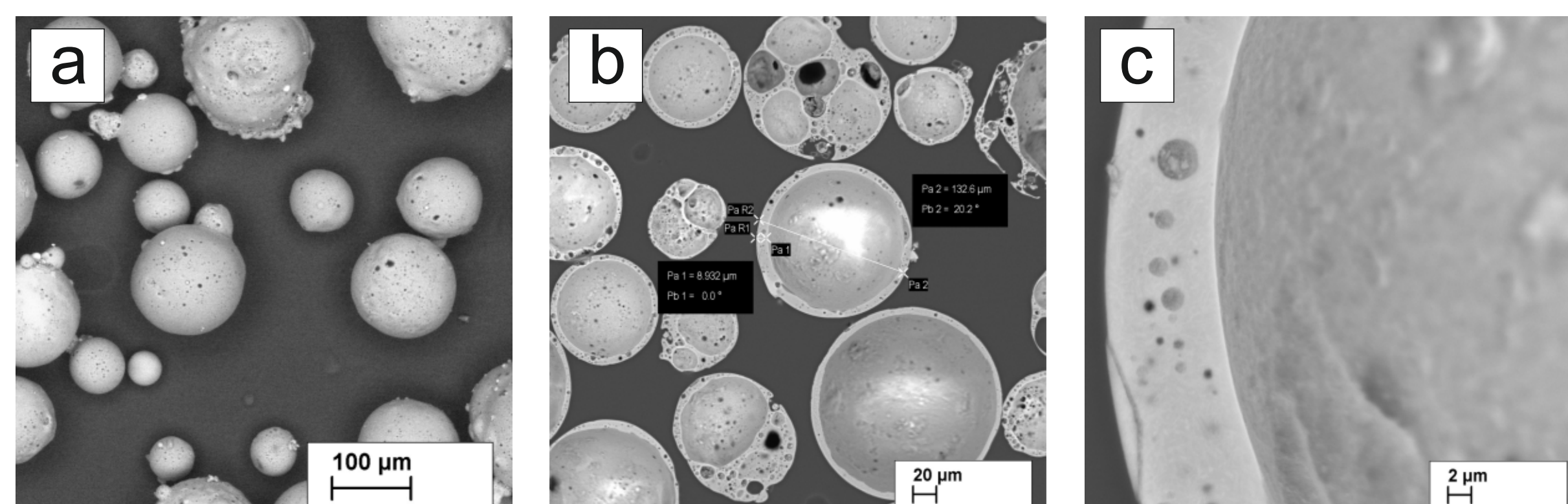


**Figure 1.** SEM images of Cenosphere: common view at X 200 times magnification (a) cross-section (b) at 500 and X 2000 (c) times magnification.

**Table 1.** Granulometric composition of used cenospheres

Sieves. mm	0.160	0.125	0.090	0.063	0.045	0.020	0.010	0.005	0.002	-0.002	d <sub>50</sub>
Mass %	0	0.3	22.8	61.7	9.1	5	0.8	0.2	0.1	0	0.0790

**Table 2.** Chemical composition of CS

Composition, mass. %									Mass loss, %	
SiO <sub>2</sub>	Al <sub>2</sub> O <sub>3</sub>	Fe <sub>2</sub> O <sub>3</sub>	CaO	MnO	Na <sub>2</sub> O	K <sub>2</sub> O	TiO <sub>2</sub>		20-400 C°	400-1000 C°
53.8	40.7	1	1.4	0.6	0.5	0.4	-		0.4	0.9



Cenosphere (CS)



**PVD**



**SPS**

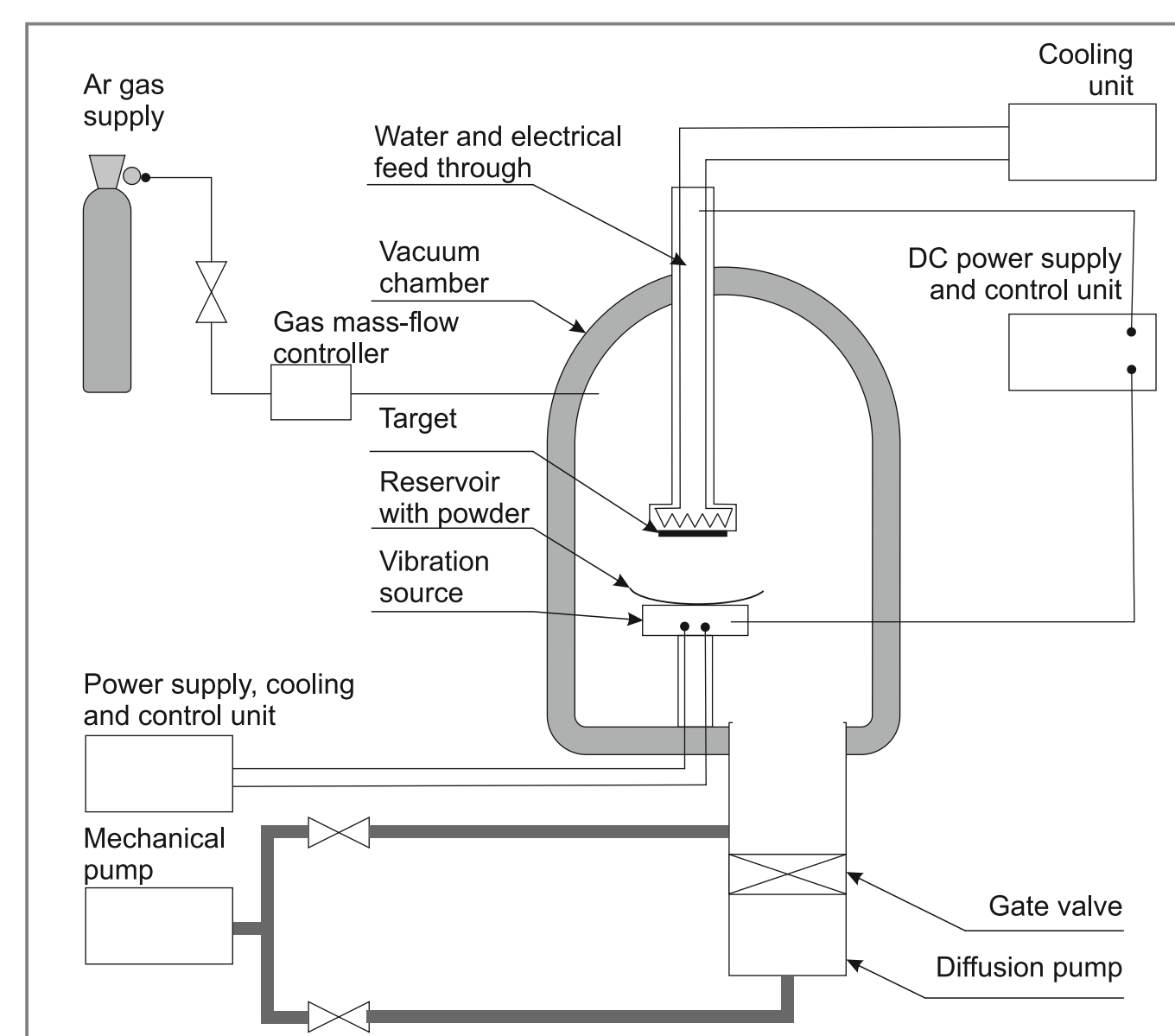


**Figure 2.** The scheme of the experimental setup of magnetron sputtering equipment for powder materials.

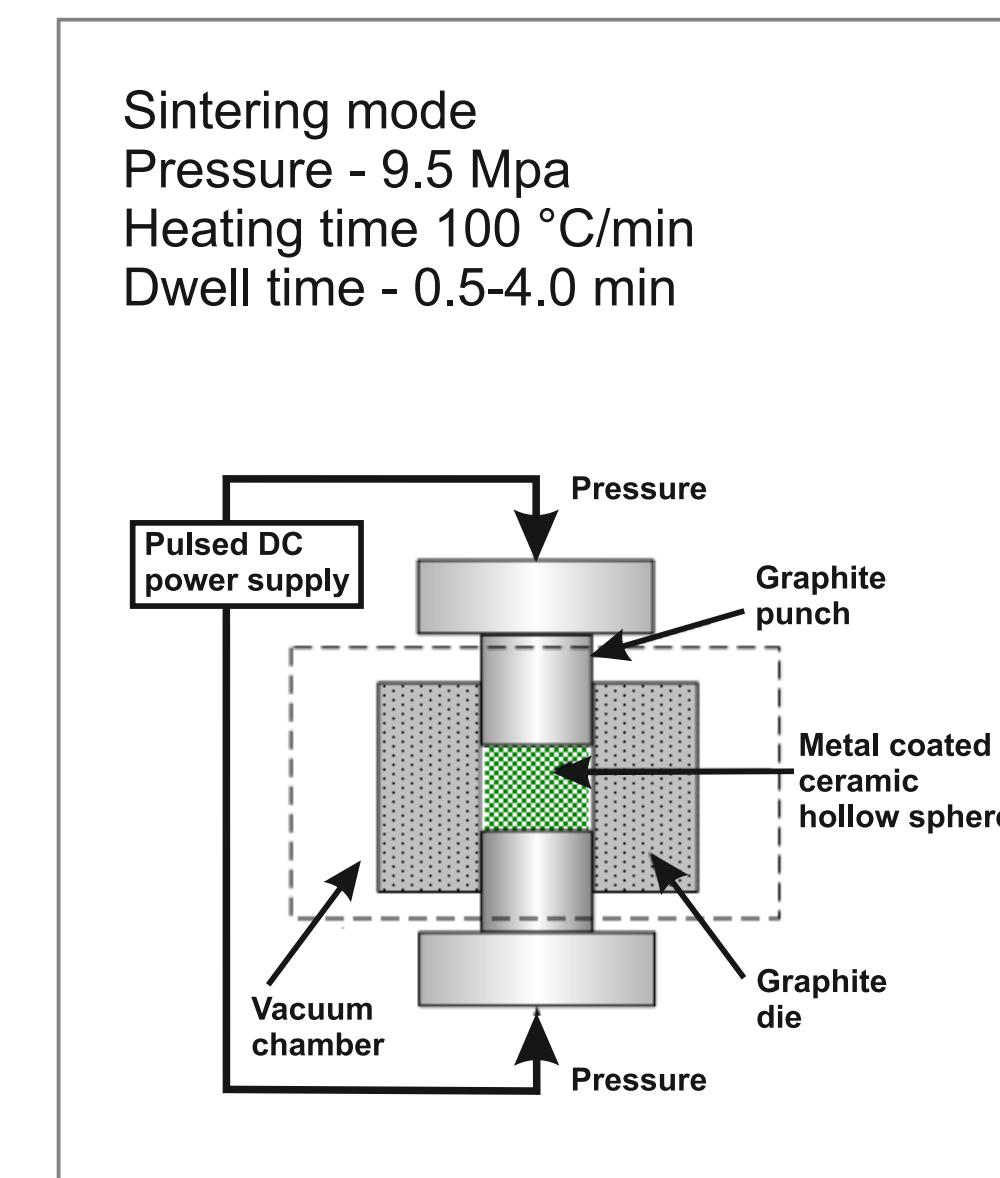


**Figure 3.** Principal scheme of the SPS experimental setup

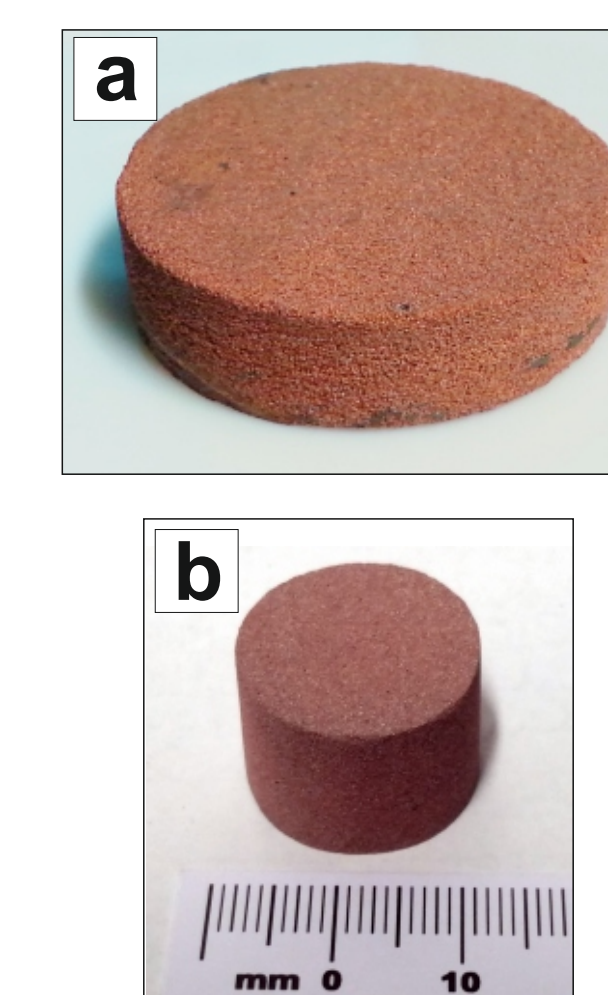


**Figure 4.** By SPS sintered specimens d=30 mm; h = 8mm (a) d=19 mm; h = 18mm (b)

## RESULTS AND DISCUSSIONS

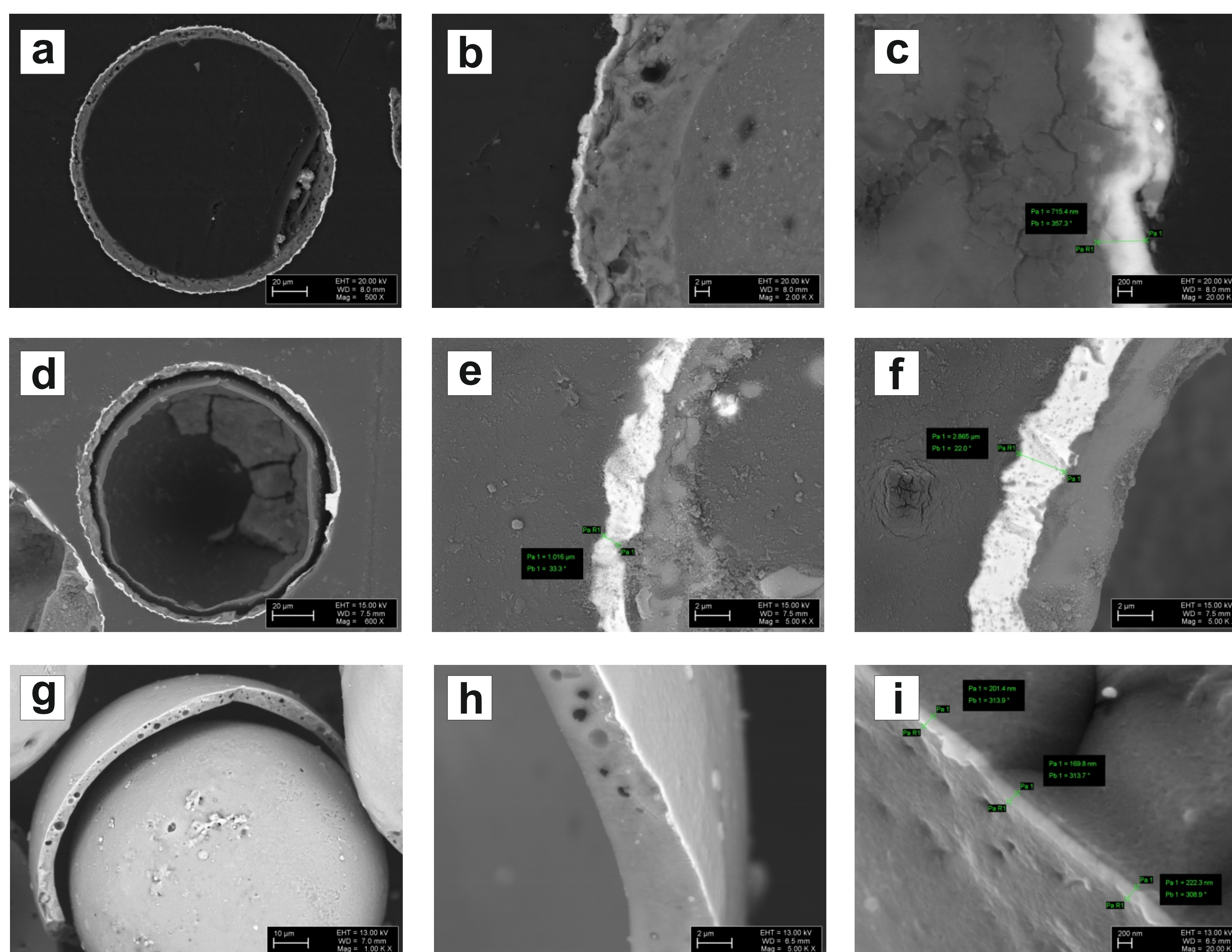


**Figure 5.** SEM (BE) images of cross-section of a composite powder: Cu@CS-6.25 a) x500, b) x5000, c) x20000 times magnification; Cu@CS-12.5 d) x600, e) x5000, f) x5000 times magnification; SS@CS-12.5 g) x1000, h) x5000, i) x20000 times magnification

### Coating thickness and CP bulk density

Three portions by 120 g of CS were treated in a magnetron sputtering machine (fig.2) at 6.25 kWh and 12.5 kWh for coating by Cu samples designated Cu@CS-6.25 and Cu@CS-12.5 respectively and at 12.5 kWh of sputtering energy for the stainless steel coating, designated as SS@CS-12.5. According to numerous measurements, the thickness of the Cu layer in Cu@CS-6.25 samples varied from 0.4 μm to 1.2 μm (fig 5a-5c), in Cu@CS-12.5 sample from 1.0 μm to 2.5 μm (fig 5e,5f) and the SS film thickness 0.2-0.8 μm (fig 5h-5i). CS wall thicknesses varied between 5μm and 15μm. In order to determinate the real amount of deposited metals the powder bulk density was measured. The composite powder Cu@CS-6.25 had bulk density 0.442±0.003 g/cm<sup>3</sup>, Cu@CS-12.5 had a bulk density 0.514±0.002 g/cm<sup>3</sup> and the SS@CS-12.5 had 0.423±0.002 g/cm<sup>3</sup>. For comparison the raw material (uncoated CS) had a bulk density 0.390±0.003 g/cm<sup>3</sup>. For the Cu coating that data has good correlation with for sputtering spent energy 6.25 kWh, 12.50 kWh and coating thickness: weight increase is 13.3% and 31.8% respectively.

### Coating morphology.

The analysis of numerous SEM images of Cu@CS-6.25 and Cu@CS-12.5 shows no difference in surface morphology. All coatings as fo Cu and for the stainless steel is uniform and non-porous. On the fig 5 is shown cross-sections of the Cu@CS-6.25 and Cu@CS-12.5 samples. Fig 5a and 5d images demonstrates complete coating of CS by Cu. A close look - fig 5c and 5e shows thickness variation on one particle from 0.7 μm to 1.4 μm for the Cu@CS-6.25 and from 1.0 μm to 2.6 μm for the Cu@CS-12.5 powders. Another situation take place with SS coating: it is less rough and less thick (fig 5h) and less thickness variation.

### By SPS sintered samples

In this step Cu@CS12.5 and SS@CS12.5 powders were used. A series of composite SF cylindrical samples (diameter 19.5 mm, height 19.5 mm) and tablets (19.5 mm, height 4 mm) were prepared by spark plasma sintering. The bulk density of the obtained samples varied in the ranges of 0.75-0.95 g/cm<sup>3</sup> and 1.0-1.4 g/cm<sup>3</sup> for Cu and SS-coated, respectively. The total porosity was 60-65% for Cu@CS and 50-53% for SS@CS. The compression strength was 15-30 MPa for Cu@CS composite. Fig 4 demonstrates Cu@CS composite - it is mechanically strong, crack free, and could be easily machined. In fig 6a the same part is shown after dry polishing with 3000 grit sandpaper. Visible white and light grey areas are the inner surface of CS, however a lot of intact CS is visible as well. It means that inter particle binding is not very strong. In case of intact CS if during grinding particle was removed completely but not broke off we can conclude that particle adhesion force is smaller than particle destruction energy. In case of opened CS binding was energy much higher than it was necessary for CS crushing. Ratio of intact/opened CS (during grinding) indicates the intensity of particle binding in the composite. In fig. 6c (SS@CS sample) quantity of crushed CS is significantly higher – almost all of CS were opened in comparison with Cu@CS (fig. 4b) This suggests better interparticle adhesion in the SS composite than in Cu composite. The electric conductivity of Cu@CS composite was 1.4•10<sup>5</sup> – 3.0•10<sup>5</sup> S/m, which belongs to conductive materials.

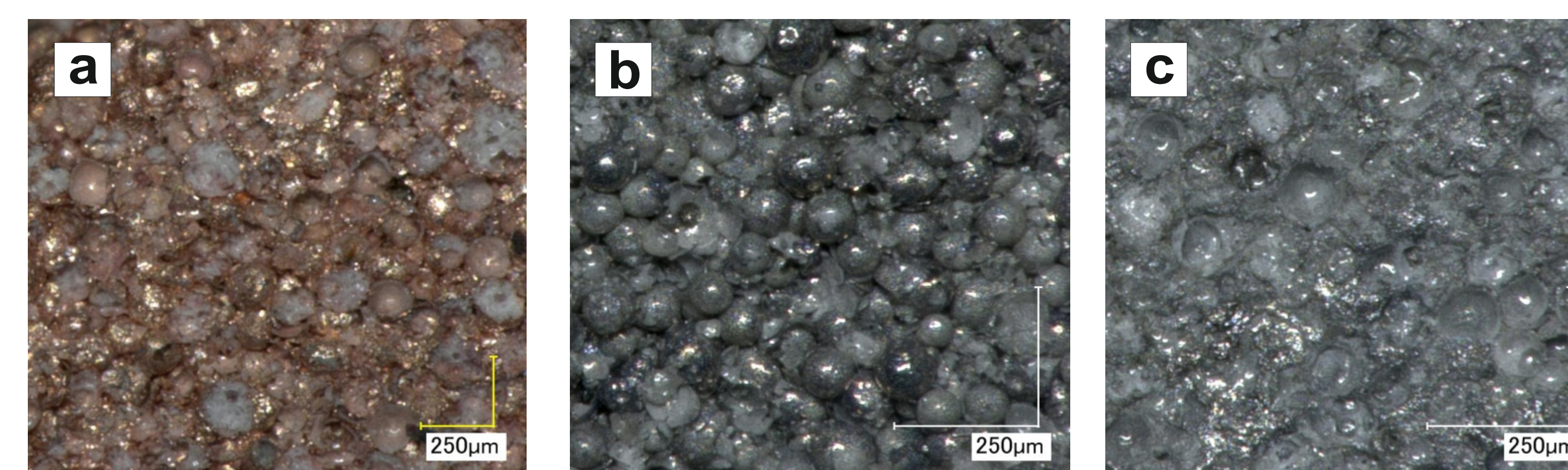


**Figure 6.**

Optical images of obtained parts by SPS method using  
a) Cu@CS (12,5 kWh)  
b) CS@CS (12,5 kWh)  
c) SS@CS (12,5 kWh) polish  
at magnification X 200 times

